

RESEARCH ARTICLE

# Novel pedigree analysis implicates DNA repair and chromatin remodeling in multiple myeloma risk

Rosalie G. Waller<sup>1</sup>✉, Todd M. Darlington<sup>1</sup>✉, Xiaomu Wei<sup>2</sup>, Michael J. Madsen<sup>1</sup>, Alun Thomas<sup>1</sup>, Karen Curtin<sup>1</sup>, Hilary Coon<sup>1</sup>, Venkatesh Rajamanickam<sup>1</sup>, Justin Musinsky<sup>3</sup>, David Jayabalan<sup>2</sup>, Djordje Atanackovic<sup>1</sup>, S. Vincent Rajkumar<sup>4</sup>, Shaji Kumar<sup>4</sup>, Susan Slager<sup>4</sup>, Mridu Middha<sup>5</sup>, Perrine Galia<sup>6</sup>, Delphine Demangel<sup>6</sup>, Mohamed Salama<sup>1</sup>, Vijai Joseph<sup>3</sup>, James McKay<sup>7</sup>, Kenneth Offit<sup>3</sup>, Robert J. Klein<sup>5</sup>, Steven M. Lipkin<sup>2</sup>, Charles Dumontet<sup>8</sup>, Celine M. Vachon<sup>4</sup>, Nicola J. Camp<sup>1\*</sup>

**1** University of Utah School of Medicine, Salt Lake City, Utah, United States of America, **2** Weill Cornell Medical College, New York, New York, United States of America, **3** Memorial Sloan Kettering Cancer Center, New York, New York, United States of America, **4** Mayo Clinic, Rochester, Minnesota, United States of America, **5** Icahn School of Medicine at Mount Sinai, New York, New York, United States of America, **6** ProfileXpert, Lyon, France, **7** International Agency for Research on Cancer, Lyon, France, **8** INSERM 1052/CNRS 5286/UCBL, Lyon, France

✉ These authors contributed equally to this work.

\* [nicola.camp@hci.utah.edu](mailto:nicola.camp@hci.utah.edu)



 OPEN ACCESS

**Citation:** Waller RG, Darlington TM, Wei X, Madsen MJ, Thomas A, Curtin K, et al. (2018) Novel pedigree analysis implicates DNA repair and chromatin remodeling in multiple myeloma risk. *PLoS Genet* 14(2): e1007111. <https://doi.org/10.1371/journal.pgen.1007111>

**Editor:** Michael P. Epstein, Emory University, UNITED STATES

**Received:** March 29, 2017

**Accepted:** November 10, 2017

**Published:** February 1, 2018

**Copyright:** © 2018 Waller et al. This is an open access article distributed under the terms of the [Creative Commons Attribution License](https://creativecommons.org/licenses/by/4.0/), which permits unrestricted use, distribution, and reproduction in any medium, provided the original author and source are credited.

**Data Availability Statement:** The Shared Genome Segment (SGS) analysis software is freely available and can be accessed online: <https://uofuhealth.utah.edu/huntsman/labs/camp/analysis-tool/shared-genomic-segment.php>. Data used in the SGS case-study analysis includes pedigree structures, myeloma diagnoses, and genome-wide SNP genotypes. Pedigree structures necessary for these analyses were acquired from the Utah Population Database (UPDB). These are considered potentially identifiable by the Resource for Genetic and Epidemiologic Research (RGE) –

## Abstract

The high-risk pedigree (HRP) design is an established strategy to discover rare, highly-penetrant, Mendelian-like causal variants. Its success, however, in complex traits has been modest, largely due to challenges of genetic heterogeneity and complex inheritance models. We describe a HRP strategy that addresses intra-familial heterogeneity, and identifies inherited segments important for mapping regulatory risk. We apply this new Shared Genomic Segment (SGS) method in 11 extended, Utah, multiple myeloma (MM) HRPs, and subsequent exome sequencing in SGS regions of interest in 1063 MM / MGUS (monoclonal gammopathy of undetermined significance—a precursor to MM) cases and 964 controls from a jointly-called collaborative resource, including cases from the initial 11 HRPs. One genome-wide significant 1.8 Mb shared segment was found at 6q16. Exome sequencing in this region revealed predicted deleterious variants in *USP45* (p.Gln691\* and p.Gln621Glu), a gene known to influence DNA repair through endonuclease regulation. Additionally, a 1.2 Mb segment at 1p36.11 is inherited in two Utah HRPs, with coding variants identified in *ARID1A* (p.Ser90Gly and p.Met890Val), a key gene in the SWI/SNF chromatin remodeling complex. Our results provide compelling statistical and genetic evidence for segregating risk variants for MM. In addition, we demonstrate a novel strategy to use large HRPs for risk-variant discovery more generally in complex traits.

the ethical oversight committee for the UPDB. As a result, access to these data requires review by the RGE committee (contact Jahn Barlow, [jahn.barlow@utah.edu](mailto:jahn.barlow@utah.edu)). Upon RGE approval, we will provide the genotypes and pedigree structure in a format ready to be used by the SGS software. Exome variants within the shared segments identified by the SGS analysis have been provided in a variant call format (VCF) file in the Supporting Information, along with an accompanying ID file describing phenotype and pedigree membership. Sporadic myeloma cases and unaffected controls were obtained with approval from the database of Genotypes and Phenotypes (dbGaP). Exome sequences can be requested through dbGaP (<https://www.ncbi.nlm.nih.gov/gap>) with the following accessions: phs000348.v2.p1, phs000748.v4.p3, phs000209.v13.p3, phs000276.v2.p1, phs000179.v5.p2, phs000298.v3.p2, phs000424.v6.p1, phs000653.v2.p1, phs000687.v1.p1, phs000814.v1.p1, and phs000806.v1.p1.

**Funding:** Research reported in this publication was supported by funding from the Utah Genome Project, <http://healthsciences.utah.edu/utah-genome-project/>, (NJC); Utah Hematology Disease Oriented Team, <https://healthcare.utah.edu/huntsmancancerinstitute/research/disease-oriented-research-teams/hematologic-malignancies-dot.php>, (NJC); Leukemia and Lymphoma Society, <https://www.lls.org/>, grant number 6067-09 (NJC); and National Institutes of Health (NIH), <https://www.nih.gov/>, grant numbers: R01-CA-107476 (SVR), R01-CA-134674 (NJC), R21-CA-152336 (NJC), R01-CA-163353 (NJC), R01-CA-167824 (SML), R01-CA-168762 (SVR), R21-CA-191896 (CMV), R01-DK-091374, R01-DK-093151, R01-MH-094400 (HC), R01-MH-099134 (HC), S10-OD-018522, and T15-LM-007124. Partial support for all datasets within the Utah Population Data Base is provided by the Huntsman Cancer Institute (HCI), <http://www.huntsmancancer.org/>, and the HCI Cancer Center Support grant, P30-CA-42014 from the NIH. The Utah Cancer Registry is funded by the National Cancer Institute's SEER Program, Contract No. HHSN2612013000171, with additional support from the Utah Department of Health, <http://health.utah.gov/>, and the University of Utah, <https://www.utah.edu>. The research reported in this publication was supported in part by the National Center for Advancing Translational Sciences of the National Institutes of Health under Award Number UL1TR001067. The content is solely the responsibility of the authors and does not necessarily represent the official views of the National Institutes of Health. The funders had no role in study design, data collection and analysis,

## Author summary

Although family-based studies demonstrate inherited variants play a role in many common and complex diseases, finding the genes responsible remains a challenge. High-risk pedigrees, or families with more disease than expected by chance, have aided discovery of genes responsible for less complex diseases, but high-risk pedigrees have not reached their potential in complex diseases. Here, we describe a method to utilize high-risk pedigrees to discover risk-genes in complex diseases. Our method is appropriate for complex diseases because it allows for genetic-heterogeneity, or multiple causes of disease, within a pedigree. This method allows us to identify shared segments that likely harbor disease-causing genes in a family. We apply our method in Myeloma, a heritable and complex cancer of plasma cells. We identified two genes *USP45* and *ARID1A* that fall within shared segments with compelling statistical evidence. Exome sequencing of these genes revealed likely-damaging variants inherited in Myeloma high-risk families, suggesting these genes likely play a role in development of Myeloma. Our Myeloma findings demonstrate our high-risk pedigree method can identify genetic regions of interest in large high-risk pedigrees that are also relevant to smaller nuclear families and overall disease risk. In sum, we offer a strategy, applicable across phenotypes, to revitalize high-risk pedigrees in the discovery of the genetic basis of common and complex disease.

## Introduction

Rare risk variants have been suggested as a source of missing heritability in the majority of complex traits [1–3]. High-risk pedigrees (HRPs) are a mainstay for identifying rare, highly penetrant, Mendelian-like, causal variants [4–11]. However, while HRP have been successful for relatively simple traits, genetic heterogeneity remains a major obstacle that reduces the effectiveness of HRP for gene mapping in complex traits [12,13]. Also challenging is mapping regulatory variants, likely to be important for complex traits, necessitating interrogation outside the well-annotated, coding regions of the genome [14,15]. Localizing chromosomal regions to target the search for rare, risk variants will be instrumental in mapping them.

Here we develop a HRP strategy based on our previous Shared Genomic Segment (SGS) approach [16] that focuses on pedigrees sufficiently large to singularly identify segregating chromosomal segments of statistical merit. The method addresses genetic heterogeneity by optimizing over all possible subsets of studied cases in a HRP. Key to the utility of the method is the derivation of significance thresholds for interpretation. These thresholds address the genome-wide search and the multiple testing inherent from the optimization through use of distribution fitting and the Theory of Large Deviations.

We apply this novel method to 11 MM HRP, and use exome sequencing from a collaborative resource of 55 multiplex MM or MM/MGUS pedigrees to perform subsequent targeted searches at the variant level. MM is a complex cancer of the plasma cells with 30,330 new cases annually (incidence 6.5/100,000 per year) [17]. Despite survival dramatically increasing from 25.8% in 1980 to 48.5% in 2012, MM remains a cancer with one of the lowest 5-year survival rates in adult hematological malignancies [17]. MM is preceded by a condition referred to as monoclonal gammopathy of undetermined significance (MGUS). Evidence for the familial clustering of MM is consistently replicated [18–21], as is its clustering with MGUS [22–25]. Genetic pedigree studies in MM are scarce as it remains a challenge to acquire samples in pedigrees due to rarity and low survival rates. The Utah MM HRP are one of only a few pedigree

decision to publish, or preparation of the manuscript.

**Competing interests:** The authors have declared that no competing interests exist.

resources worldwide and contains unparalleled multi-generational high-risk pedigrees. Thus far, no segregating risk variants have been identified for MM.

## Results

### Pedigree analysis strategy

We developed a gene mapping strategy, based on the SGS method [16,26], that accounts for intra-familial heterogeneity and multiple testing. The basic SGS method identifies all genomic segments shared identical-by-state (sharing without regard to inheritance) between a defined set of cases using a dense genome-wide map of common single nucleotide polymorphisms (SNPs), either from a genotyping platform or extracted from sequence data. If the length of a shared segment is significantly longer than by chance, inherited sharing is implied; theoretically, chance inherited sharing in distant relatives is extremely improbable. Nominal chance occurrence (nominal p-value) for shared segments is assessed empirically using gene-drop simulations to create a null distribution, as follows. Null genotype configurations are generated by assigning haplotypes to pedigree founders according to a publicly available linkage disequilibrium (LD) map. These null genotypes are segregated through the pedigree structure to the case set via simulated Mendelian inheritance according to a genetic (recombination) map. (Gene-drops are performed independent of disease status.) The resulting genotype data in the case set are representative of chance sharing. This basic method was shown to have excellent power in homogeneous pedigrees [16].

In our new strategy, we address heterogeneity within pedigrees in a “brute-force” fashion by iterating over all non-trivial combinations of the cases (subsets) in each pedigree. For each subset, shared segments at every position throughout the genome are identified and nominal p-values assigned. Across subsets, an optimization procedure is performed, at every marker across the genome, to identify the segment with the most significant sharing evidence. All shared segments selected by the optimization procedure, and their respective p-values, comprise the final optimized SGS results for a pedigree.

To perform significance testing and identify segments that are unexpected by chance (hypothesized to harbor risk loci), we derive significance thresholds to account for the genome-wide optimization. Acknowledging that the vast majority of observed sharing across a genome is under the null (true risk loci are a very small minority of the genome), we use the observed optimized results ( $Y = -\log_{10}(p)$ , where  $p$  is the nominal p-value) to model the distribution for optimized SGS results. We note that this approach may be slightly conservative because signals for true risk loci are also included. We identified the gamma distribution as adequate to represent the distribution (Fig 1). Based on the fitted distribution,  $Y \sim \Gamma(k, \sigma)$ , where  $k$  and  $\sigma$  are the shape and rate parameters, we apply the Theory of Large Deviations—previously applied to successfully model genome-wide fluctuations in linkage analysis [27]. The significance threshold,  $T$ , accounts for multiple testing of optimized segments across the genome, and is found by solving Eq 1:

$$\mu(X) = [C + 2GX]\alpha(X) \tag{1}$$

where  $T = 10^{-X\sigma/2}$ ,  $X = 2Y/\sigma \sim \chi_{2k}^2$ ,  $\mu(X)$  is the genome-wide false positive rate required,  $C$  is the number of chromosomes,  $\alpha(X)$  is nominal probability of exceeding  $X$ , and  $G$  is the genome length in Morgans. A criterion of  $\mu(X) = 0.05$  is used to define the genome-wide significant threshold (false positive rate of 0.05 per genome), and  $\mu(X) = 1$  to define the genome-wide suggestive threshold (false positive rate of 1 per genome).

In general, we found that the fitted distributions produced stable significance thresholds after 100,000–300,000 simulations (Table 1). Typically, threshold determination requires

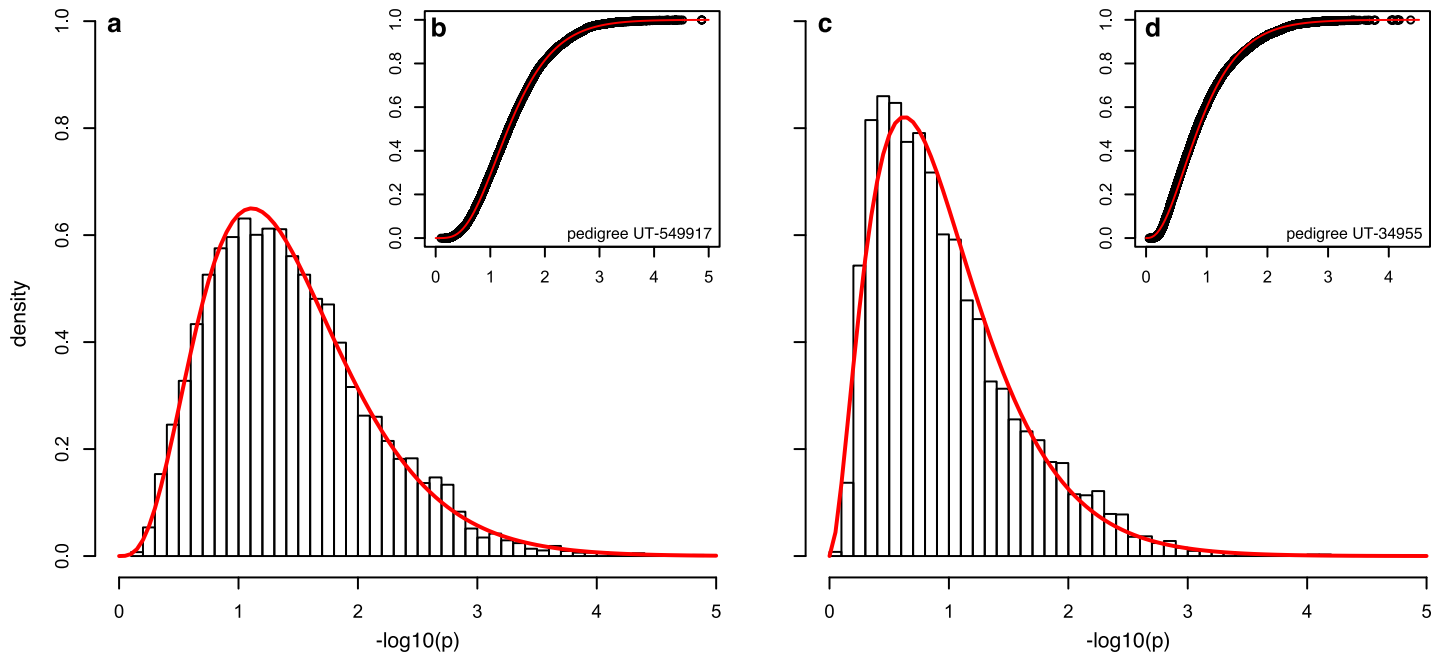


**Fig 1. Adequacy of the gamma distribution.** The gamma distribution provides an adequate fit for multiple types of pedigrees. For example, HRP UT-549917 has  $k = 4.4$  and  $\sigma = 3.6$  with good visual density (a) and CDF (b) fit, with  $\lambda = 0.9$ . (Goodness of fit was estimated with  $\lambda$ , the median of empirical chi-squared distribution divided by the median of the expected chi-squared distribution.) HRP UT-34955 has  $k = 2.8$  and  $\sigma = 2.9$  with good visual density (c) and CDF (d) fit, with  $\lambda = 1.0$ .

<https://doi.org/10.1371/journal.pgen.1007111.g001>

1,000–3,000 CPU hours per pedigree, increasing with the number of subsets and separating meioses between pedigree cases. For example, in pedigree UT-571744, 300k simulations genome-wide (2,513,408 segments) took 1,275 CPU hours on tangent nodes featuring Intel Xeon E5-2650 processors. Once significance thresholds are established, subset/segment combinations of potential interest are identified and additional simulations are restricted to those combinations to gain the required p-value resolution. For these subsequent targeted simulations, we use a marginalized LD map specific for the segment of interest, dramatically reducing the analysis time. For example, in pedigree UT-571744, 600M simulations on one segment took 325 CPU hours on tangent nodes featuring Intel Xeon E5-2650 processors. See [S1 Fig](#) for an overview of the strategy pipeline.

### Application to Utah, MM HRPs

We applied our new pedigree analysis strategy to 11 Utah MM HRPs using high-density OMNI Express SNP array genotype data. Each pedigree was selected to contain excess MM (4–37 MM total per pedigree), had 2–4 sampled MM cases with genotype data, and 8–23 meioses per pedigree between the sampled cases. After quality control, a consistent set of 678,447 SNPs were used for all SGS analyses. The total number of shared segments for each pedigree

**Table 1. Genome-wide significance thresholds.** Fitted distributions are stable enough for threshold determination after 100,000 to 300,000 simulations.

Pedigree	100k	200k	300k	1M
260	$6.36 \times 10^{-6}$	$6.35 \times 10^{-6}$	$6.28 \times 10^{-6}$	$6.25 \times 10^{-6}$
576834	$3.50 \times 10^{-6}$	$3.53 \times 10^{-6}$	$3.53 \times 10^{-6}$	$3.51 \times 10^{-6}$
571744	$3.80 \times 10^{-6}$	$3.83 \times 10^{-6}$	$3.75 \times 10^{-6}$	$3.80 \times 10^{-6}$
34955	$5.67 \times 10^{-6}$	$5.60 \times 10^{-6}$	$5.61 \times 10^{-6}$	$5.61 \times 10^{-6}$

<https://doi.org/10.1371/journal.pgen.1007111.t001>

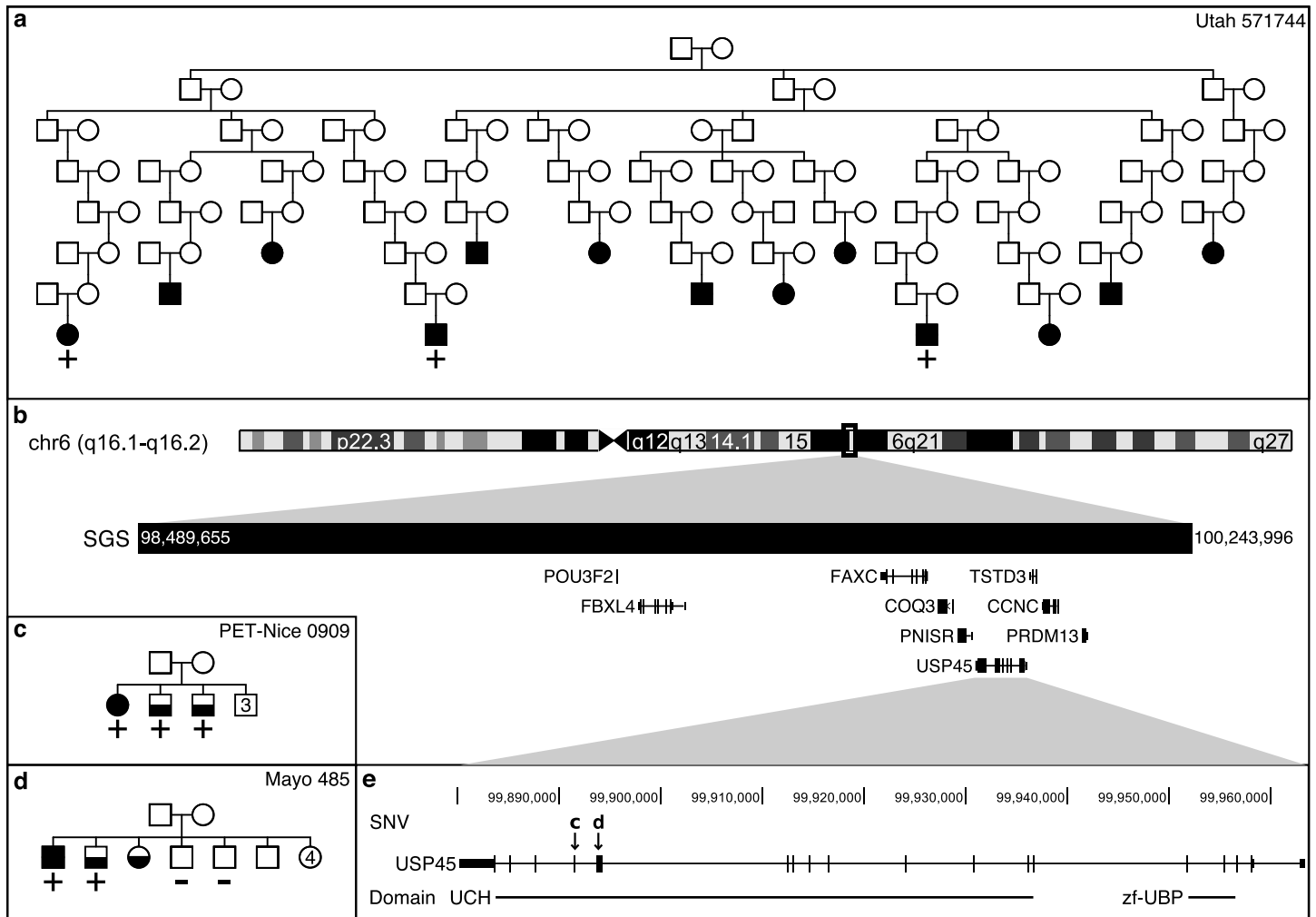


**Fig 2. Significant SGS, pedigrees, and segregating SNVs.** In pedigrees, MM cases are fully shaded and MGUS cases are half shaded. Numbers indicate multiple individuals. a) Utah pedigree, 571744, sharing the genome-wide significant SGS. The pedigree is trimmed to allow for viewing (37 MM confirmed cases are known in this pedigree, 3 were ascertained and genotyped). + indicates the genotyped MM cases that are SGS carriers, - indicates genotyped and non-carriers, no carrier status indicates not genotyped. Note—the genealogy extends beyond SEER cancer registry data. MGUS status is unknown in this pedigree. b) Genomic region of significant SGS. c) INSERM pedigree carrying the stop gain SNV marked by “c” in box e. 1 MM and 2 MGUSs carry the SNV. d) Mayo Clinic pedigree carrying the missense SNV marked by “d” in box e. 1 MM and 1 MGUS carry the SNV, but 2 unaffected siblings do not carry the SNV. e) Risk candidate gene, *USP45*, has 2 segregating SNVs in the ubiquitin C-terminal hydrolase 2 (UCH) domain.

<https://doi.org/10.1371/journal.pgen.1007111.g002>

across all subsets ranged from 638,525 to 6,765,500 (larger pedigrees with more subsets producing larger numbers of segments). After optimization,  $Y = -\log_{10}(p)$  for 6,697 to 10,369 segments were fit to gamma distributions for each pedigree, and used to determine genome-wide significant and suggestive thresholds (Eq 1). The genome-wide significant thresholds ranged from  $6.2 \times 10^{-5}$  to  $7.8 \times 10^{-7}$  and genome-wide suggestive from  $8.2 \times 10^{-4}$  to  $2.1 \times 10^{-5}$  (S1 Table).

A genome-wide significant, 1.8 Mb shared segment ( $p = 3.3 \times 10^{-6}$ ) was observed in pedigree UT-571744. All three genotyped MM cases, separated by 20 meioses, share the segment (Fig 2A and Table 2). The segment is located at chromosome 6q16 (98.49–100.24 Mb; hg19) and includes 9 genes: *POU3F2*, *FBXL4*, *FAXC*, *COQ3*, *PNISR*, *USP45*, *TSTD3*, *CCNC*, and *PRDM13* (Fig 2B).

We also identified two HRP, UT-576834 and UT-260, with overlapping borderline, genome-wide suggestive, shared segments at 1p36.11 (Fig 3). A 8.9 Mb (24.39–33.30 Mb,

**Table 2. Significant or overlapping SGSs and segregating SNVs.**

Family	Cases	Me	Position	Len	p-value	Gene	Conseq	Impact	AAF
UT-571744	3	20	6:98,489,655–100,243,996	1.8	3.3x10 <sup>-6</sup> ‡				
PET-Nice 0909	3(2)	3	6:99,891,443			USP45	p.Gln691*	SG	None
Mayo 458	2(1)	2	6:99,893,787			USP45	p.Gln621Glu	MS	None
UT-576834	3	12	1:24,389,214–33,298,821	8.9	3.0x10 <sup>-4</sup>				
UT 260	3	16	1:26,224,634–27,384,988	1.2	2.1x10 <sup>-4</sup>				
UT-576834	3	12	1:27,023,162 <sup>^</sup>			ARID1A	p.Ser90Gly	MS	0.0002
Cornell MM12	2	4	1:27,089,712 <sup>^</sup>			ARID1A	p.Met890Val	MS	0.0001

**Legend:** Cases—number of MM and MGUS cases (number of MGUS) with genotype or exome DNaseq data who share the SGS region or carry the SNV; Me—meioses; Position—build HG19, <sup>^</sup>rs752026201, <sup>^</sup>rs140664170; Len—length in mega-bases; p-value for SGS (significant and suggestive genome-wide thresholds were 3.8x10<sup>-6</sup> and 8.5x10<sup>-5</sup> for UT-571744, 3.5x10<sup>-6</sup> and 4.6x10<sup>-5</sup> for UT-576834, and 6.2x10<sup>-6</sup> and 1.2x10<sup>-4</sup> for UT 260)

‡genome-wide significant; Conseq—exome-variant consequence; SG—stop gain variant, MS—missense variant; AAF—alternate allele frequency based on the non-TCGA, non-Finnish, European gnomAD individuals. “None” indicates the region has good coverage, but the variant has not been observed in gnomAD, while an AAF = 0 indicates the variant has been observed in another ethnicity.

<https://doi.org/10.1371/journal.pgen.1007111.t002>

p = 3.0x10<sup>-4</sup>) segment was observed in 3 of the 4 genotyped MM cases in UT-576834, shared across 12 meioses (Fig 3B and Table 2). A nested 1.2 Mb shared segment (26.22–27.38 Mb; p = 2.1x10<sup>-4</sup>) segregated to 3 MM cases separated by 16 meioses in UT-260 (Fig 3A and Table 2). The overlapping segment contains 30 genes (Fig 3D).

### Exome follow-up of shared segments in HRP

Whole-exome sequencing (WES) data was interrogated, targeted to the identified SGS region, to identify potential risk variants in the pedigree sharers in the HRP and in a broader set of 44 pedigrees. WES data was available for: 28 cases from the 11 extended Utah HRP; and 126 exomes from 44 densely clustered MM/MGUS families from Mayo Clinic Rochester, Weill Cornell, Memorial Sloan Kettering Cancer Center, International Agency for Research on Cancer, and INSERM France (S2 Table). Prioritization was used to identify variants that were: in the target segment; rare (alternate allele frequency, AAF<0.001 in the non-Finnish, European, gnomAD individuals), potentially deleterious (variant impact predicted to be high or moderate); and observed recurrently in the appropriate segment sharers (if observed in the segment discovery pedigree).

At 6q16, no rare, potentially deleterious coding risk variants were shared by the 3 UT-571744 MM cases in the 1.8 Mb genome-wide significant segment, indicating non-coding regulatory variants may be responsible for MM risk in this pedigree. However, two, rare coding and potentially deleterious single nucleotide variants (SNVs) were identified in two MM/MGUS families (Fig 2C–2E and Table 2). Both SNVs are in the hydrolase domain of USP45: a stop gain (p.Gln691\*) shared by 3 sibling cases (1 MM and 2 MGUS) in an INSERM family (PET-Nice 0909) and a missense SNV (p.Gln621Glu) shared by 2 siblings (1 MM and 1 MGUS) but not their 2 screened unaffected siblings in Mayo family 485. Coverage of these positions in ExAC sequence data is high (> 99% of the 60,706 ExAC samples had at least 10x read coverage) and neither variant was observed. Collating the SGS evidence in UT-571744 (genome-wide rate of  $\mu = 0.042$ ) with the sequence findings, correcting for 11 SGS pedigrees, the 45 pedigrees interrogated for sequence variants, and the 9 genes in the SGS region, we estimate the rate of observing all these findings at the 6q16 region by chance is very low ( $\pi = 0.0026$ , see Methods) and study-wide significant.

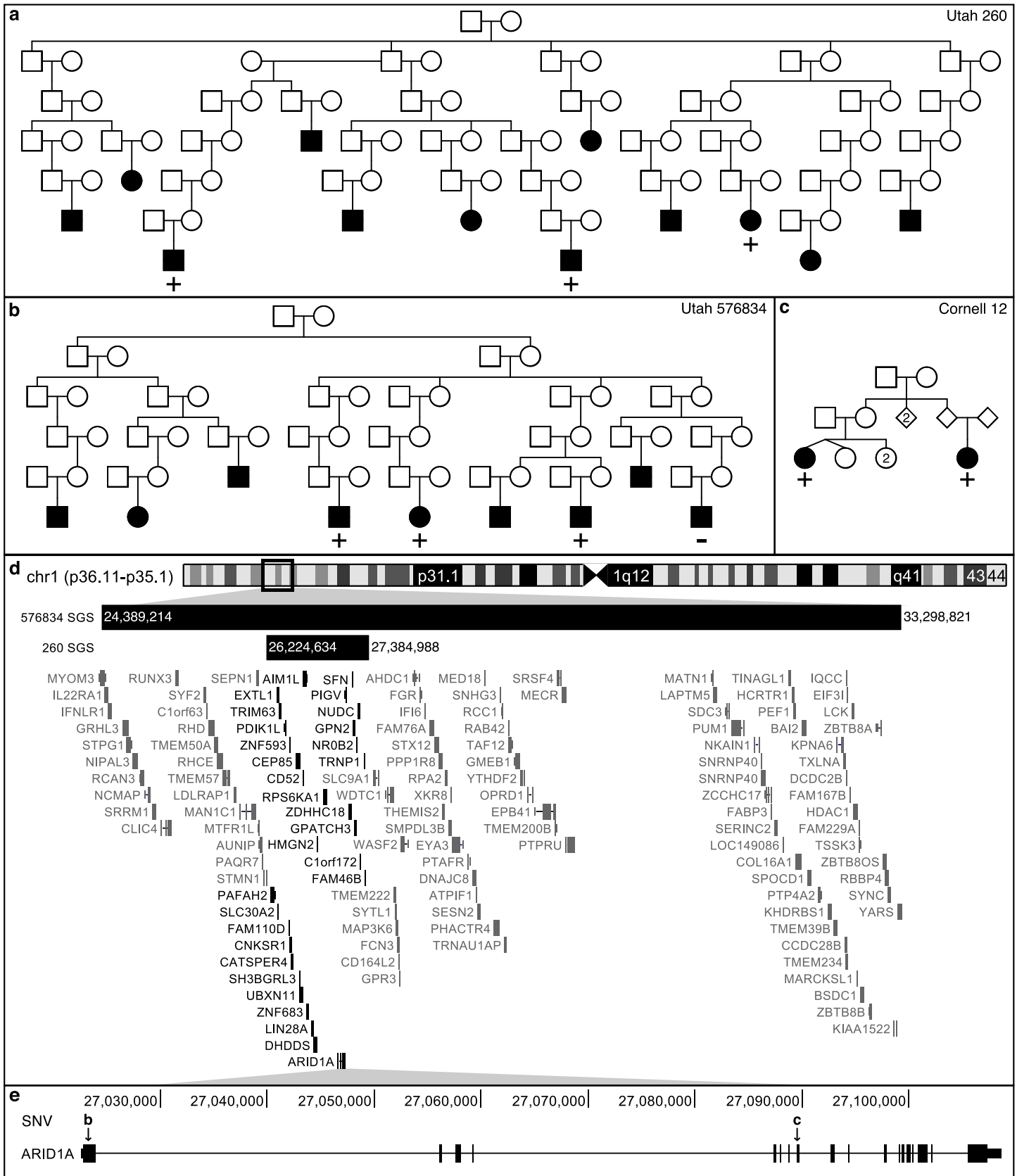


**Fig 3. SGS with multiple lines of evidence.** a/b) Utah pedigrees carrying the overlapping SGSs on chr1p36.11-p35.1. + indicates the genotyped MM cases that are SGS carriers, – indicates genotyped and non-carriers, no carrier status indicates not genotyped. c) Weill Cornell pedigree with a segregating, missense SNV in *ARID1A* indicated by “c” in box e. d) Genomic region of overlapping SGS. Dark black genes fall in both regions. e) 2 rare and segregating, missense SNVs were observed in whole-exome sequencing. SNV “b” is carried by the cases indicated with + in box b. SNV “c” is carried by the cases in box c.

<https://doi.org/10.1371/journal.pgen.1007111.g003>

Pedigree exomes in the 1.2 Mb segment at 1p36.11 revealed two, rare and potentially deleterious SNVs. The first in discovery pedigree UT-576834: a missense SNV (rs752026201, p.Ser90Gly, AAF = 0.0002 in gnomAD) in *ARID1A* (Fig 3E) shared by 3 of the 4 Utah MM cases, concordant with the segment sharing pattern. A second rare, missense SNV in *ARID1A* (rs140664170, p.Met890Val, AAF = 0.0001 in gnomAD) was found to be carried by a pair of MM cousins in Weill-Cornell family 12 (Fig 3C and 3E, and Table 2). No rare, potentially deleterious coding risk variants were shared by the 3 MM cases in UT-260. Based on the ExAC data, *ARID1A* is extremely intolerant to missense variants and loss of function (LoF) SNVs [28].

### Pathway follow-up of candidate genes

Our SGS findings and pedigree WES identify *USP45* and *ARID1A* as candidate genes for inherited MM risk. We further investigated shared segments and WES for evidence supporting the complexes *USP45* and *ARID1A* are involved in. Here we further expanded our WES to: 186 MM/MGUS cases (early onset MM/MGUS or familial MGUS) from our collaborative group, 733 sporadic MM cases from dbGaP [29], and 964 controls [30].

*USP45* is an essential DNA repair regulator, de-ubiquitylating ERCC1 to allow for DNA translocation of the ERCC1-ERCC4 endonuclease [31,32]. This endonuclease is a part of the global genome nucleotide-excision repair (GG-NER) incision complex, a 22 protein complex essential to removing lesions from DNA and cancer prevention [33–36] (S3 Table). We reviewed SGS results in the Utah HRP at the location of these 22 genes and identified a genome-wide suggestive segment in pedigree UT-34955 (S2 Fig). This HRP identified a 0.8 Mb segment at 19q13 (45.71–46.51 Mb; hg19), containing 31 genes including *ERCC1* and *ERCC2* (S2 Fig and S4 Table). The segment is shared by 3 MM cases separated by 16 meioses ( $p = 6.6 \times 10^{-5}$ ). No rare, coding variants were identified from the WES in the 3 MM cases in UT-34955, nor in the remaining 44 pedigrees/families. We interrogated the 23 GG-NER genes in our 919 MM/MGUS exomes. This identified a ClinVar-annotated pathogenic, missense SNV in *ERCC4* (p.Arg799Trp) in one early-onset MM case and one sporadic MM case, and a stop-gain SNV in *ERCC3* (p.Arg574Ter), in the same domain as a ClinVar-annotated pathogenic variant, in a second early-onset MM case (S4 Table). Further, burden testing in all MM cases vs controls was significant in 2 of the 23 GG-NER genes: *GTF2H1* and *DDB1* after correcting for multiple testing (S3 Table). The occurrence of two significantly burdened genes (at  $\alpha = 0.0022$ ) from 23 genes is unexpected ( $p = 0.0011$ , Binomial(23,0.0022)).

*ARID1A* is a member of the SWI/SNF chromatin remodeling complex, a 15 gene complex involved in DNA transcription regulation [37] (see S5 Table). Members of this complex are mutated in >20% of malignancies [38–40], but are extremely intolerant to LoF and missense variation [41] (S5 Table). We reviewed SGS results in the Utah HRP at the location of these 15 genes and identified a borderline genome-wide suggestive segment in pedigree UT-549917 shared by 4 MM cases across 21 meioses ( $p = 2.17 \times 10^{-5}$ , S3 Fig and S6 Table). This 1.5 Mb segment at chr3p21.1-p21.2 (52.01–53.56 Mb; hg19) contains 32 genes including *PBRM1* from the SWI/SNF complex. No coding variants were identified in this gene in UT-549917, nor in the remaining 44 pedigrees/families. Burden testing was significant for 7 of the 15 genes in the complex after correcting for multiple testing: *ARID1A*, *ARID1B*, *SMARCA4*, *ACTL6A*,



*SMARCD3*, *SMARCC2*, and *SMARCE1* (S5 Table). The occurrence of seven significantly burdened genes (at  $\alpha = 0.0033$ ) from 15 genes is unexpected by chance ( $p = 2.7 \times 10^{-14}$ , Binomial (15,0.0033)).

## Discussion

We developed a novel strategy to identify segregating chromosomal segments shared by subsets of cases in HRP. It focuses on extended HRP that are singularly powerful to identify significant genetic segregation. Our strategy allows for genetic heterogeneity within such pedigrees and provides formal significance thresholds for valid interpretation. Previously, extended HRP have not delivered on their potential in complex traits because in common, complex traits, HRP are likely enriched for multiple susceptibility variants and may capture both familial and sporadic cases in their branches. Our optimization strategy over subsets is attractive because it allows for heterogeneity without prior knowledge of genetic similarities or deep phenotyping. This new statistic also identifies the sharers and clearly delimits the shared region, making follow-up interrogation straight-forward. This is a distinct advantage over standard linkage analysis and previous pairwise SGS methods where neither sharers or the region are defined [42].

Application of the method to extended MM pedigrees demonstrated the utility of this new method and illustrated that the segments identified were used successfully to narrow the search for risk variants in smaller pedigrees, allowing for an overall strategy that can utilize both large pedigrees and smaller families together for discovery (Table 2, Fig 2 and Fig 3). Post-hoc, additional value can be gained from demographic and/or clinical data on the sharing subsets shedding light on other shared characteristics that may aid future mapping. Also, we note that in the absence of any significant findings, genome-wide SGS results can be used as genomic annotations of segregation evidence for more heuristic approaches.

While we identified several rare, potentially deleterious coding variants of interest, several of the SGS discovery pedigrees had no coding variants that satisfied prioritization criteria. We believe this will be characteristic of complex traits and that regulatory variants will also play a substantial role. Mutations with strong causal likelihood found in other disease cohorts may focus the search for regulatory variation to particular genes within a shared segment, as with *USP45* in MM. In the absence of such compelling evidence, a return to pedigree segregation methods will provide identification of statistically compelling regions which can concentrate efforts to identify and characterize regulatory risk variants. Future work will include targeted sequencing of the promising MM SGS identified to investigate non-coding variants that may play a role in MM risk in these families. Our proposed method is a new analytic tool with the potential to reinvigorate the use of extended HRP in the identification of risk variants that contribute to common, complex disease.

Multiple myeloma is a malignancy of the plasma cells that has been shown to be familial [43]. Consistent with a role for genetics, case-control studies have been successful in identifying association signals for 17 low-risk variants [44–48]. However, despite consistent evidence for familial clustering, our study is the first to explore high-risk MM pedigrees. Using the unique genealogical database available in Utah, we identified and studied extended MM HRP. We identified a genome-wide significant segment containing *USP45*, an important regulator of DNA repair (Fig 2 and Table 2), and a genome-wide suggestive segment harboring other genes in the GG-NER incision complex (*ERCC1* and *ERCC2*). Exome sequencing in a collaborative resource of high-risk families and early-onset cases revealed four rare, potentially deleterious coding variants; two novel variants in *USP45* segregating in two pedigrees and two variants in early-onset cases in *ERCC3* and *ERCC4*, the latter annotated as pathogenic in

ClinVar. Burden testing including sporadic MM, and comparing to controls, identified significant enrichment for variants in MM cases in 2 of the 23 GG-NER genes in the protein endonuclease regulation complex.

In particular, the functional literature supports *USP45* as a candidate cancer risk gene. *USP45* has been shown to deubiquitylate ERCC1, a catalytic subunit of the ERCC1-ERCC4 DNA repair endonuclease (ERCC4 also known as XPF) [31]. This endonuclease is a critical regulator of DNA repair processes [34]. The complex repairs recombination, double strand break, and inter-strand crosslink by cutting DNA overhangs around a lesion, degrades 3' G-rich overhangs in telomere maintenance, and plays a role in cancer prevention and in tumor resistance to chemotherapy [31,34]. Mouse models have shown *USP45* knockout cells have higher levels of ubiquitylated ERCC1 and that cells are hypersensitive to UV radiation and DNA inter-strand cross-links, repair of UV-induced DNA damage, and ERCC1 translocation to DNA damage is impaired [31]. Hence, the deubiquitylase activity of *USP45* is important for maintaining the DNA repair ability of ERCC1-ERCC4. In total, these observations implicate the GG-NER incision complex and specifically the interaction of *USP45* and the disruption of the ERCC1-ERCC4 role in DNA repair as a mechanism of potential importance in MM risk.

Our strategy also identified shared segments overlapping at chr1p36.11 in two Utah pedigrees containing *ARID1A* (Fig 3 and Table 2) and a borderline genome-wide suggestive segment in a third pedigree harboring another gene in the SWI/SNF complex (*PBRM1*). For the SWI/SNF complex, exome sequencing revealed two rare, potentially deleterious variants in *ARID1A* segregating in two pedigrees. Burden testing provided further evidence for enrichment of variants in *ARID1A* specifically, and in 7 of the 15 genes in the complex. As a component of the SWI/SNF chromatin remodeling complex, *ARID1A* facilitates gene activation by assisting transcription machinery gain access to gene targets [49]. Based on the patterns of mutations in tumor cells, *ARID1A* likely functions as a tumor-suppressor [50]. Members of the SWI/SNF chromatin remodeling complexes are mutated in 20% of malignancies [38], but are extremely intolerant to LoF and missense variation [41] (S5 Table). Blockage of chromatin remodeling may sustain cancer development [39]. Aberrant chromatin remodeling contributes to the pathogenesis of ovarian clear-cell carcinoma [50]. It has previously been shown that *ARID1A* is intolerant to variation (LoF and missense mutations) [28], consistent with its prominent somatic role in multiple tumors [38,50,51], including hematological malignancies [52–54]. These observations implicate the SWI/SNF chromatin remodeling complex, and specifically *ARID1A* in MM risk.

This study has limitations. First, the method is applicable only to extended HRP that are singularly effective for identifying segregating segments (15 meioses between cases is optimal [16]). The method is not directly applicable to the many smaller family-based resources that have been gathered in the complex trait field and may therefore result in findings from single large pedigrees that are private and difficult to replicate. However, as illustrated in our example, in a collaborative setting containing both extended HRP and smaller families, the approach can be mutually beneficial. Second, our observation of two borderline genome-wide suggestive overlapping segments at 1p36 led to our identification of *ARID1A* as a potential candidate risk gene and illustrates the potential for discoveries using overlapping subthreshold evidence. However, it raises analytical questions of how to systematically identify such segments. This segment would have been ignored based on strict individual-pedigree thresholds and highlights an important area for further methodological development. Third, as in all family-based genetic studies our method is susceptible to inaccurate pedigree structures and poorly matched control populations. However, relationship and ethnicity checks are standard protocol and mitigate the possibility of error. Finally, this study is observational and cannot describe causation. We have identified two complexes, several genes and specific variants as

compelling candidates involved in MM risk, but further functional studies will be required to determine and characterize the mechanisms involved in risk.

In conclusion, we have developed a strategy for gene mapping in complex traits that accounts for heterogeneity within HRP and formally corrects for multiple testing to allow for statistically rigorous discovery. We applied this strategy to MM, a complex cancer of plasma cells, and identified multiple shared segments containing genes in nucleotide excision repair and SWI/SNF chromatin remodeling. Exome follow-up supported these segments in both the Utah large HRP and smaller families from other sites. Our study offers a novel technique for HRP gene mapping and demonstrates its utility to narrow the search for risk-variants in complex traits.

## Methods

### Ethics statement

Human subjects research was performed with informed written consent, under protocols approved by ethics committees for: University of Utah (protocol 29801), Memorial Sloan Kettering (protocols 06–107 and 00–069), Comité de Protection des Personnes-SUD EST IV (protocols ID-RCB N° 2007-A00644-49 and DGS2007-0547), Mayo Clinic (protocols 489–04, 2128–05 and 1465–04), International Agency for Research on Cancer (protocol 12–19), and Weill-Cornell (protocol 0010004608).

### SGS analysis in Utah, Myeloma HRP

**HRPs and genotyping.** All participants were studied with informed consent under protocols approved by the University of Utah IRB. Using the statewide Utah Cancer Registry (UCR), all living individuals with MM in Utah were invited to participate and peripheral blood was collected for DNA extraction. Participants were linked in the Utah Population Database (UPDB), a unique resource that integrates UCR records with a 5M person genealogy. HRP were defined as pedigrees containing statistical excess of MM ( $p < 0.05$ ), based on sex and cohort-specific rates in Utah. Eleven of the HRP identified in the UPDB contained 3 or 4 MM cases with DNA (total MM cases per pedigree ranged from 4 to 37) with 8 to 23 meioses between studied MM cases. DNA from the 28 cases was genotyped on the Illumina Omni Express high-density SNP array.

**Quality control.** Only bi-allelic SNPs were considered. Genotypes and individual call-rates were used to ensure high quality data. PLINK was used to remove SNPs with  $< 95\%$  call rate across individuals [55]. The final SNP set contained 678,447 single nucleotide variants. After SNP removal for low call rates, individuals were removed based on  $< 90\%$  call rate across the genome, or if they failed the PLINK sex check. One MM case was removed. The QC'd SNP data were transformed to match strand orientation of the 1000Genomes. PLINK relationship estimates were assessed against pedigree structure from the UPDB to identify any potential issues with pedigree structure. None were found.

**Probability of sharing a segment.** SGS analysis identifies contiguous SNPs that are shared identical-by-state (IBS) by cases in a HRP and assigns an empirical probability of chance ancestral sharing [26]. First, a set of cases in a HRP are defined and all segments of contiguous SNPs shared IBS are identified. All shared segments  $> 20$  SNPs are considered. Lengths shorter than 20 are commonly shared between unrelated individuals. Second, population-based data (here we used CEU and GBR data from the 1000Genomes Project [56]) are used to estimate a graphical model for linkage disequilibrium (LD) [57], providing a probability distribution of chromosome-wide haplotypes in the population. Third, pairs of haplotypes are randomly assigned to pedigree founders according to the haplotype distribution. Founders

are individuals whose parents are not specified in the pedigree. For chromosome-wide haplotype simulations the full chromosome LD model is used. Fourth, Mendelian segregation and recombination are simulated to generate genotypes for all pedigree members. The Rutgers genetic map [58] is used for a genetic map for recombination, with interpolation based on physical base pair position for SNPs not represented. Steps two through four create one simulated data set, a random sample from the null hypothesis. This process is repeated hundreds of thousands to millions of times for each subset.

Each shared segment in the real data (step one) is compared to the simulated segments at the precise genomic location. The number of times the null segment equals or encompasses the observed segment is counted and divided by the total number of simulations to generate the empirical nominal p-value for the observed shared segment. The simulations continue until a p-value has been estimated to a required resolution, or until it surpasses a defined significance threshold. To facilitate this in an efficient manner, we follow-up specific segments using marginal distributions from the LD model, established using standard graphical modeling methods [59]. The marginalized LD model encompassing only the region of interest, but capturing relevant LD to accurately simulate genotypes from this region alone. This reduction in markers vastly increases the speed in which simulations are generated. The graphical model estimation, marginalization, and simulation processes are computationally efficient requiring time and storage that is linear with the number of SNPs being considered.

**Heterogeneity optimization.** We systematically perform SGS analysis on each subset of cases in a HRP. If required, the number of subsets can be limited by meioses or subset size. This may be necessary for common traits with large full sets. A lower limit of 10 meioses is a good rule of thumb for reducing the computational burden of subset assessment. At each marker position across the genome, the optimized segment is the one minimizing the p-value across all subsets considered. All segments selected by the optimization procedure, and their respective p-values, comprise the final optimized SGS results.

**Significance threshold determination.** A transformation,  $Y = -\log_{10}(p)$  is performed to the optimized genome-wide SGS p-value vector. The results are fit to a gamma distribution using the MLE method.  $Y \sim \Gamma(k, \sigma)$  ( $k$  shape,  $\sigma$  rate parameterization). The Theory of Large Deviations has previously been used in pedigree studies to model extreme values in a genome-wide genetic setting [27], and it has been shown that for a statistic following a Gaussian distribution, the number of segments where the statistic exceeds a threshold  $W$  has mean:

$$\mu(W) = [C + 2\rho GW^2]\alpha(W), \tag{2}$$

where  $\alpha(W)$  is the pointwise significance level of exceeding  $W$ ,  $C$  is the number of chromosomes considered,  $\rho$  reflects the recombination rate ( $\rho = 1$  for general pedigrees), and  $G$  is genetic length in Morgans. Lander & Kruglyak demonstrated that the same equation extends a statistic following the chi-squared distribution:

$$\mu(X) = [C + 2\rho GX]\alpha(X), \tag{3}$$

based on the distributional relationship between the chi-squared and Normal distributions  $W^2 = X$ . Here, we use the distributional relationship between the gamma and chi-square distributions, our estimated  $k$  and  $\sigma$  gamma parameters, where  $T = 10^{-X\sigma/2}$ ,  $X = 2Y/\sigma \sim \chi_{2k}^2$ , and the genetic length of the genome (matched to that used in the gene-drop) to utilize Eq 3 and derive  $\mu(X)$  thresholds. Solving for  $\mu(X) = 0.05$  and  $\mu(X) = 1$  produced significance and suggestive thresholds, respectively. These thresholds are remarkably stable after a few hundred thousand simulations. For pedigrees with very large numbers of meioses (>50) between the full case-set, a larger number of simulations may be required.

**Software availability.** The SGS program is available for download at <http://healthsciences.utah.edu/huntsman/labs/camp/analysis-tool/shared-genomic-segment.php>. The main architecture is written in Java. Probability assessments can be multi-threaded, but the largest parallelization gains are achieved by running independent analyses across chromosomes.

## Targeted sequencing

**Participants.** WES data were interrogated in the regions defined by the shared segments of interest. WES data was available on 964 controls [30] and 1,063 MM or MGUS cases including: 28 MM from the 11 Utah HRP; 70 MM and 46 MGUS from 44 densely clustered families (each containing at least 2 MM or at least 1 MM and 1 MGUS); 186 genetically-enriched MM/MGUS (148 MM and 38 MGUS) including early-onset and MGUS clustering in families; and 733 sporadic MM cases from dbGaP [29]. Of the 44 densely clustered, MM/MGUS high-risk families, 25 were ascertained by INSERM, France (36 MM, 38 MGUS), 9 by Mayo Clinic, Minnesota (10 MM, 8 MGUS, 10 unaffected family members), 6 by Memorial Sloan Kettering Cancer Center, New York (14 MM), 3 by International Agency for Research on Cancer, France (8 MM), and 1 by Weill Cornell, New York (2 MM). Most of the families had both MM and MGUS cases (32 families total) and 12 families only had MM cases sequenced. Six families had at least one unaffected relative sequenced. (See S2 Table) All individuals in the Utah HRP and all but three of the densely clustered families were of non-Finish European descent.

**Joint calling analysis.** To perform joint calling of all of the exome sequences, we utilized the calling pipeline developed at the Icahn School of Medicine at Mt. Sinai, based on GATK Best Practices [60]. Briefly, FASTQ files were aligned to genome build 37 using bwa version 0.7.8, indels were realigned using GATK, duplicates were removed using Picard MarkDuplicates, and base quality scores were recalibrated using GATK. HaplotypeCaller was then used to generate individual GVCF files for each individual, and GenotypeGVCFs was used to generate the final joint calling. The jointly-called VCF was annotated with SNPEff and loaded into a GEMINI (GENome MINing) database for ease of querying [61]. Some additional functional annotations available in the GEMINI suite include CADD, ANNOVAR, conservation, location, and if the variant was listed in OMIM.

**Variant prioritization.** A GEMINI query was developed to identify variants which were: high or medium impact; AAF < 0.001 in the non-Finnish, European, gnomAD individuals; and within the shared segments of interest. Genes harboring segregating variants in at least two high-risk pedigrees (the discovery pedigree and/or the 44 high-risk pedigrees from collaborating sites) were considered candidate susceptibility genes. These criteria were selected to maintain findings that were unlikely by chance.

**Framework for joint assessment of pedigree findings (SGS and sequencing).** Here we present a framework to provide an estimate for a study-wide rate of observing SGS regions and sequence variants. These approximations are presented to provide some statistical perspective of the observed findings to guide interpretation.

The first stage is SGS analyses in the Utah pedigrees. As described above, SGS results are assessed against significance thresholds which account for the multiple testing across the genome and the optimization over subsets. This step is a formal statistical assessment and provides a fully corrected rate ( $\mu$ ) of observing an SGS region per pedigree; for example,  $\mu = 0.05$  indicates a region that would be expected to be observed once in 20 genomes by chance, and is referred to as genome-wide significant (see “Significance threshold determination”, above).

The second stage is prioritization of genes based on observed sequence variants in pedigrees. For this step, we interrogated the region defined by the SGS analysis; both in the Utah

pedigree that generated the region, and in an independent set of (smaller) pedigrees from our collaborators (44 pedigrees). We prioritized genes where at least two rare ( $AAF \leq 0.001$ ), HIGH/MED impact sequence variants were observed in the same gene in two pedigrees; each variant shared by multiple cases in each pedigree. In ExAC exomes, 3,563,315 variants have VEP annotation for HIGH or MED impact severity variant [28]. These arise from 60,706 individuals (121,412 chromosomes) across 26,724 genes [28]. Additionally, ~99% are  $< 0.01$ , and ~72% are not seen in the 1000G (i.e. frequency  $< 0.001$ ) [28]. From these ExAC observations we can estimate that on average there are 0.0008 HIGH/MED variants observed with  $AAF < 0.001$  per chromosome per gene ( $= (3,563,315 \times 0.72) / (121,412 \times 26,724)$ ).

In the pedigree that defined an SGS region (i.e., where segregation of the region to  $n$  cases has already been defined), sequencing in the  $n$  cases amounts to sequencing  $(n+1)$  different chromosomes and thus  $(n+1)$  chances to observe a variant of interest. However, only  $1/(n+1)$  times will the variant reside by chance on the segregating chromosome. Hence, the probability of observing a segregating variant of interest is  $(n+1) \times 0.0008 \times 1/(n+1)$ , which is 0.0008. In the independent set of 44 small pedigrees, the simplest structure is a sib-pair. In a sib-pair there are 4 parental chromosomes to observe a variant of interest, and the chance probability it is inherited to both siblings is 0.25, which also leads to an overall occurrence of sharing of 0.0008 ( $= 4 \times 0.0008 \times 0.25$ ). More distant relatives lead to less likely chance sharing. Hence, we can conservatively model the number of segregating rare, MED/HIGH impact severity variants,  $V$ , observed by chance in 45 pedigrees by a Binomial distribution,  $V \sim \text{Bin}(45, 0.0008)$ . Based on this distribution, the probability of observing at least two rare, HIGH/MED impact segregating variants in the same gene is  $\phi = P(V \geq 2) = 6.2 \times 10^{-4}$ . We can use a simple Bonferroni adjustment to account for the  $G$  genes in the SGS region.

Finally, for  $N$  SGS pedigrees in the initial stage, there are  $N$  opportunities to discover SGS regions. Hence, the overall rate of an SGS finding plus sequence variant findings within the SGS region can be approximated by  $\pi = N \times \mu \times \phi \times G$ . Where  $\pi \leq 0.05$ , this indicates study-wide significance accounting for chance findings across both stages and all multiple testing. Assuming a genome-wide significant SGS result ( $\mu = 0.05$ ), and  $N = 11$  SGS pedigrees,  $\pi$  remains below 0.05 for  $G < 147$ . Hence, in general, our protocol to define a candidate gene as one with 2 segregating rare ( $AAF \leq 0.001$ ), HIGH/MED sequence variants within a significant SGS region will generally lead to discoveries that are unexpected by chance (provided the SGS contains less than 147 genes). In particular, for our most significant chromosome 6 SGS finding ( $\mu = 0.042$  and  $G = 9$ ) the overall combined study-wide rate is  $\pi = 0.0026$  ( $11 \times 0.042 \times 0.00062 \times 9$ ).

**Burden testing.** Based on the candidate genes generated from the pedigree findings (*USP45* and *ARID1A*), burden testing was performed on jointly called and processed WES from 1,063 MM/MGUS cases and 964 unaffected controls for the 23 genes in the GG-NER incision complex (including *USP45*) and 15 genes in the SWI/SNF chromatin remodeling complex. The GEMINI software [61] was used to perform a  $c$ -alpha test [62] with 1,000 permutations. Only variants with  $AAF < 0.05$  and high or moderate predicted impact were included in the analysis.

## Supporting information

**S1 Fig. SGS analysis workflow.** Overview of the strategy pipeline. Genotypes can be generated from a high-density SNP array, or by extracting SNVs from whole-genome sequencing. CEU and GBR genotypes (unrelated individuals only) from the 1000Genomes Project are generally used as population controls. Dotted boxes represent steps done per-pedigree. Dash-dot boxes represent steps done on all subsets of cases within a pedigree. Dashed box contains step

repeated for each simulation. Abbreviations: SNP—single nucleotide polymorphism; SGS—shared genomic segment; LD—linkage disequilibrium; PED—pedigree file (contains relationships and genotypes).

(EPS)

**S2 Fig. Genome-wide suggestive segment contains *ERCC1*.** a) Utah pedigree carrying the genome-wide suggestive SGS at chr19q13.32. + indicates the genotyped MM cases that are SGS carriers, — indicates genotyped and non-carriers, no carrier status indicates not genotyped. b) Genomic region captured by the SGS. *ERCC1* and *ERCC2* are contained.

(EPS)

**S3 Fig. Shared segment containing *PBRM1*.** a) Pedigree Utah 549917 carries a genome-wide suggestive SGS at chr3p21.2-p21.1. + indicates the genotyped MM cases that are SGS carriers, — indicates genotyped and non-carriers, no carrier status indicates not genotyped. b) Genome region captured by the SGS including *PBRM1*, a component of the SWI/SNF chromatin remodeling complex.

(EPS)

**S1 Table. Genome-wide thresholds and segments.**

(PDF)

**S2 Table. Whole-exome sequenced families.** Total MM, MGUS, and controls in each pedigree and from each site.

(PDF)

**S3 Table. GG-NER Incision Complex genes.** Burden testing results (based on 1,063 MM/MGUS cases and 964 unaffected controls), SGS and prioritized SNV results, and intolerance to missense and loss of function variants (based on ExAC population data).

(PDF)

**S4 Table. Evidence for endonuclease regulation of DNA repair.**

(PDF)

**S5 Table. SWI/SNF Complex genes.** Burden testing results (based on 1,063 MM/MGUS cases and 964 unaffected controls), SGS and prioritized SNV results, and intolerance to missense and loss of function variants (based on ExAC population data).

(PDF)

**S6 Table. Evidence for SWI/SNF chromatin remodeling.**

(PDF)

**S1 File. Phenotype and pedigree membership details of samples used to explore sequence variants in SGS regions.**

(TXT)

**S2 File. Exome variants (meeting requirements in Methods section, Variant Prioritization) within the shared segments.**

(VCF)

## Acknowledgments

We thank the DNA Sequencing Core Facility and Genomics Core Facility at the University of Utah, and the computational resources and staff expertise provided by Scientific Computing at the Icahn School of Medicine at Mount Sinai. Data collection was made possible, in part, by

the Utah Population Database and the Utah Cancer Registry. We thank the participants and their families who make this research possible.

## Author Contributions

**Conceptualization:** Rosalie G. Waller, Todd M. Darlington, Nicola J. Camp.

**Data curation:** Rosalie G. Waller, Todd M. Darlington, Xiaomu Wei, Karen Curtin, Venkatesh Rajamanickam, Justin Musinsky, David Jayabalan, Djordje Atanackovic, Shaji Kumar, Mridu Middha, Perrine Galia, Delphine Demangel, Vijai Joseph, James McKay, Robert J. Klein, Steven M. Lipkin, Charles Dumontet, Celine M. Vachon, Nicola J. Camp.

**Formal analysis:** Rosalie G. Waller, Xiaomu Wei, Michael J. Madsen, Karen Curtin, Robert J. Klein.

**Funding acquisition:** Steven M. Lipkin, Charles Dumontet, Celine M. Vachon, Nicola J. Camp.

**Investigation:** Rosalie G. Waller, Todd M. Darlington, Xiaomu Wei, Michael J. Madsen, Robert J. Klein, Steven M. Lipkin, Charles Dumontet, Celine M. Vachon, Nicola J. Camp.

**Methodology:** Rosalie G. Waller, Todd M. Darlington, Michael J. Madsen, Alun Thomas, Hilary Coon, Nicola J. Camp.

**Project administration:** Rosalie G. Waller, Steven M. Lipkin, Charles Dumontet, Celine M. Vachon, Nicola J. Camp.

**Resources:** James McKay, Robert J. Klein, Steven M. Lipkin, Charles Dumontet, Celine M. Vachon, Nicola J. Camp.

**Software:** Rosalie G. Waller, Todd M. Darlington, Michael J. Madsen, Alun Thomas, Nicola J. Camp.

**Supervision:** S. Vincent Rajkumar, Susan Slager, Mohamed Salama, Kenneth Offit, Steven M. Lipkin, Celine M. Vachon, Nicola J. Camp.

**Validation:** Rosalie G. Waller, Todd M. Darlington, Steven M. Lipkin, Charles Dumontet, Celine M. Vachon, Nicola J. Camp.

**Visualization:** Rosalie G. Waller, Todd M. Darlington, Nicola J. Camp.

**Writing – original draft:** Rosalie G. Waller, Todd M. Darlington, Nicola J. Camp.

**Writing – review & editing:** Rosalie G. Waller, Todd M. Darlington, Xiaomu Wei, Michael J. Madsen, Alun Thomas, Karen Curtin, Hilary Coon, Venkatesh Rajamanickam, Justin Musinsky, David Jayabalan, Djordje Atanackovic, S. Vincent Rajkumar, Shaji Kumar, Susan Slager, Mridu Middha, Perrine Galia, Delphine Demangel, Mohamed Salama, Vijai Joseph, James McKay, Kenneth Offit, Robert J. Klein, Steven M. Lipkin, Charles Dumontet, Celine M. Vachon, Nicola J. Camp.

## References

1. Maher B. Personal genomes: The case of the missing heritability. *Nature*. 2008; 456: 18–21. <https://doi.org/10.1038/456018a> PMID: 18987709
2. Manolio TA, Collins FS, Cox NJ, Goldstein DB, Hindorf LA, Hunter DJ, et al. Finding the missing heritability of complex diseases. *Nature*. 2009; 461: 747–53. <https://doi.org/10.1038/nature08494> PMID: 19812666



3. Eichler EE, Flint J, Gibson G, Kong A, Leal SM, Moore JH, et al. Missing heritability and strategies for finding the underlying causes of complex disease. *Nat Rev Genet.* 2010; 11: 446–50. <https://doi.org/10.1038/nrg2809> PMID: 20479774
4. Miki Y, Swensen J, Shattuck-Eidens D, Futreal PA, Harshman K, Tavtigian S, et al. A strong candidate for the breast and ovarian cancer susceptibility gene BRCA1. *Science.* 1994; 266: 66–71. Available: <http://www.ncbi.nlm.nih.gov/pubmed/7545954> PMID: 7545954
5. Wooster R, Neuhausen SL, Mangion J, Quirk Y, Ford D, Collins N, et al. Localization of a breast cancer susceptibility gene, BRCA2, to chromosome 13q12-13. *Science.* 1994; 265: 2088–90. Available: <http://www.ncbi.nlm.nih.gov/pubmed/8091231> PMID: 8091231
6. Vance JM, Pericak-Vance MA, Yamaoka LH, Speer MC, Rosenwasser GO, Small K, et al. Genetic linkage mapping of chromosome 17 markers and neurofibromatosis type I. *Am J Hum Genet.* 1989; 44: 25–9. Available: <http://www.ncbi.nlm.nih.gov/pubmed/2491777> PMID: 2491777
7. Cannon-Albright LA, Goldgar DE, Meyer LJ, Lewis CM, Anderson DE, Fountain JW, et al. Assignment of a locus for familial melanoma, MLM, to chromosome 9p13-p22. *Science.* 1992; 258: 1148–52. Available: <http://www.ncbi.nlm.nih.gov/pubmed/1439824> PMID: 1439824
8. Leppert M, Dobbs M, Scambler P, O'Connell P, Nakamura Y, Stauffer D, et al. The gene for familial polyposis coli maps to the long arm of chromosome 5. *Science.* 1987; 238: 1411–3. Available: <http://www.ncbi.nlm.nih.gov/pubmed/3479843> PMID: 3479843
9. Nishisho I, Nakamura Y, Miyoshi Y, Miki Y, Ando H, Horii A, et al. Mutations of chromosome 5q21 genes in FAP and colorectal cancer patients. *Science.* 1991; 253: 665–9. Available: <http://www.ncbi.nlm.nih.gov/pubmed/1651563> PMID: 1651563
10. Ng SB, Buckingham KJ, Lee C, Bigham AW, Tabor HK, Dent KM, et al. Exome sequencing identifies the cause of a mendelian disorder. *Nat Genet.* 2010; 42: 30–5. <https://doi.org/10.1038/ng.499> PMID: 19915526
11. Ng SB, Bigham AW, Buckingham KJ, Hannibal MC, McMillin MJ, Gildersleeve HI, et al. Exome sequencing identifies MLL2 mutations as a cause of Kabuki syndrome. *Nat Genet.* 2010; 42: 790–3. <https://doi.org/10.1038/ng.646> PMID: 20711175
12. McClellan J, King M-C. Genetic Heterogeneity in Human Disease. *Cell.* 2010; 141: 210–217. <https://doi.org/10.1016/j.cell.2010.03.032> PMID: 20403315
13. Mitchell KJ. What is complex about complex disorders? *Genome Biol.* 2012; 13: 237. <https://doi.org/10.1186/gb-2012-13-1-237> PMID: 22269335
14. Li X, Montgomery SB. Detection and Impact of Rare Regulatory Variants in Human Disease. *Front Genet.* 2013; 4. <https://doi.org/10.3389/fgene.2013.00067> PMID: 23755067
15. Albert FW, Kruglyak L. The role of regulatory variation in complex traits and disease. *Nat Rev Genet.* 2015; 16: 197–212. <https://doi.org/10.1038/nrg3891> PMID: 25707927
16. Knight S, Abo RP, Abel HJ, Neklason DW, Tuohy TM, Burt RW, et al. Shared Genomic Segment Analysis: The Power to Find Rare Disease Variants. *Ann Hum Genet.* 2012; 76: 500–509. <https://doi.org/10.1111/j.1469-1809.2012.00728.x> PMID: 22989048
17. Myeloma—SEER Stat Fact Sheets [Internet]. Available: <https://seer.cancer.gov/statfacts/html/mulmy.html>
18. Cannon-Albright LA, Thomas A, Goldgar DE. Familiality of cancer in Utah. *Cancer Res.* 1994; 54: 2378–2385. PMID: 8162584
19. Landgren O, Linet MS, McMaster ML, Gridley G, Hemminki K, Goldin LR. Familial characteristics of autoimmune and hematologic disorders in 8,406 multiple myeloma patients: A population-based case-control study. *Int J Cancer.* 2006; 118: 3095–3098. <https://doi.org/10.1002/ijc.21745> PMID: 16395700
20. Albright F, Teerlink C, Werner TL, Cannon-Albright LA. Significant evidence for a heritable contribution to cancer predisposition: a review of cancer familiality by site. *BMC Cancer.* BioMed Central Ltd; 2012; 12: 138. <https://doi.org/10.1186/1471-2407-12-138> PMID: 22471249
21. Schinasi LH, Brown EE, Camp NJ, Wang SS, Hofmann JN, Chiu BC, et al. Multiple myeloma and family history of lymphohaematopoietic cancers: Results from the International Multiple Myeloma Consortium. *Br J Haematol.* England; 2016; 175: 87–101. <https://doi.org/10.1111/bjh.14199> PMID: 27330041
22. Landgren O, Kristinsson SY, Goldin LR, Caporaso NE, Blimark C, Mellqvist U-H, et al. Risk of plasma cell and lymphoproliferative disorders among 14621 first-degree relatives of 4458 patients with monoclonal gammopathy of undetermined significance in Sweden. *Blood.* 2009; 114: 791–5. <https://doi.org/10.1182/blood-2008-12-191676> PMID: 19182202
23. Greenberg AJ, Rajkumar SV, Vachon CM. Familial monoclonal gammopathy of undetermined significance and multiple myeloma: epidemiology, risk factors, and biological characteristics. *Blood.* 2012; 119: 5359–66. <https://doi.org/10.1182/blood-2011-11-387324> PMID: 22354002

24. Greenberg AJ, Rajkumar SV, Larson DR, Dispenzieri A, Therneau TM, Colby CL, et al. Increased prevalence of light chain monoclonal gammopathy of undetermined significance (LC-MGUS) in first-degree relatives of individuals with multiple myeloma. *Br J Haematol*. 2012; 157: 472–5. Available: <http://www.ncbi.nlm.nih.gov/pubmed/22629552> PMID: 22629552
25. Vachon CM, Kyle RA, Therneau TM, Foreman BJ, Larson DR, Colby CL, et al. Increased risk of monoclonal gammopathy in first-degree relatives of patients with multiple myeloma or monoclonal gammopathy of undetermined significance. *Blood*. 2009; 114: 785–90. <https://doi.org/10.1182/blood-2008-12-192575> PMID: 19179466
26. Thomas A, Camp NJ, Farnham JM, Allen-Brady K, Cannon-Albright LA. Shared Genomic Segment Analysis. Mapping Disease Predisposition Genes in Extended Pedigrees Using SNP Genotype Assays. *Ann Hum Genet*. 2008; 72: 279–287. 10.1111/j.1469-1809.2007.00406.x <https://doi.org/10.1111/j.1469-1809.2007.00406.x> PMID: 18093282
27. Lander E, Kruglyak L. Genetic dissection of complex traits: guidelines for interpreting and reporting linkage results. *Nat Genet*. 1995; 11: 141–147.
28. Lek M, Karczewski KJ, Minikel E V., Samocha KE, Banks E, Fennell T, et al. Analysis of protein-coding genetic variation in 60,706 humans. *Nature*. *Nature Research*; 2016; 536: 285–291. <https://doi.org/10.1038/nature19057> PMID: 27535533
29. Myeloma data downloaded from the dbGaP web site under accessions: phs000348.v2.p1 and phs000748.v4.p3. [Internet].
30. Control data downloaded from the dbGaP web site under accessions: phs000209.v13.p3, phs000276.v2.p1, phs000179.v5.p2, phs000298.v3.p2, phs000424.v6.p1, phs000653.v2.p1, phs000687.v1.p1, phs000814.v1.p1, and phs000806.v1.p1.
31. Perez-Oliva AB, Lachaud C, Szyaniarowski P, Muñoz I, Macartney T, Hickson I, et al. USP45 deubiquitylase controls ERCC1-XPF endonuclease-mediated DNA damage responses. *EMBO J*. 2015; 34: 326–43. <https://doi.org/10.15252/embj.201489184> PMID: 25538220
32. USP45 in the GG-NER Incision Complex [Internet]. Available: <http://www.reactome.org/PathwayBrowser/#/R-HSA-5696398&SEL=R-HSA-5696465&PATH=R-HSA-73894>
33. Marteijn JA, Lans H, Vermeulen W, Hoeijmakers JHJ. Understanding nucleotide excision repair and its roles in cancer and ageing. *Nat Rev Mol Cell Biol*. 2014; 15: 465–81. <https://doi.org/10.1038/nrm3822> PMID: 24954209
34. Kirschner K, Melton DW. Multiple roles of the ERCC1-XPF endonuclease in DNA repair and resistance to anticancer drugs. *Anticancer Res*. 2010; 30: 3223–3232. 30/9/3223 [pii] PMID: 20944091
35. Friedberg EC. How nucleotide excision repair protects against cancer. *Nat Rev Cancer*. 2001; 1: 22–33. <https://doi.org/10.1038/35094000> PMID: 11900249
36. Christmann M, Tomicic MT, Roos WP, Kaina B. Mechanisms of human DNA repair: an update. *Toxicology*. 2003; 193: 3–34. Available: <http://www.ncbi.nlm.nih.gov/pubmed/14599765> PMID: 14599765
37. SWI/SNF Chromatin Remodeling Complex [Internet]. Available: <http://www.reactome.org/PathwayBrowser/#/R-HSA-5696398&PATH=R-HSA-73894>
38. Biegel JA, Busse TM, Weissman BE. SWI/SNF chromatin remodeling complexes and cancer. *Am J Med Genet C Semin Med Genet*. 2014; 166C: 350–66. <https://doi.org/10.1002/ajmg.c.31410> PMID: 25169151
39. Romero O a, Sanchez-Cespedes M. The SWI/SNF genetic blockade: effects in cell differentiation, cancer and developmental diseases. *Oncogene*. *Nature Publishing Group*; 2014; 33: 2681–9. <https://doi.org/10.1038/onc.2013.227> PMID: 23752187
40. Roberts CWM, Orkin SH. The SWI/SNF complex—chromatin and cancer. *Nat Rev Cancer*. *Nature Publishing Group*; 2004; 4: 133–142. Available: <http://dx.doi.org/10.1038/nrc1273> PMID: 14964309
41. Lek M, Karczewski KJ, Minikel E V., Samocha KE, Banks E, Fennell T, et al. Analysis of protein-coding genetic variation in 60,706 humans. *Nature*. *Nature Research*; 2016; 536: 285–291. <https://doi.org/10.1038/nature19057> PMID: 27535533
42. Cai Z, Camp NJ, Cannon-Albright L, Thomas A. Identification of regions of positive selection using Shared Genomic Segment analysis. *Eur J Hum Genet*. *Nature Publishing Group*; 2011; 19: 667–671. <https://doi.org/10.1038/ejhg.2010.257> PMID: 21304558
43. Morgan GJ, Johnson DC, Weinhold N, Goldschmidt H, Landgren O, Lynch HT, et al. Inherited genetic susceptibility to multiple myeloma. *Leukemia*. 2014; 28: 518–24. <https://doi.org/10.1038/leu.2013.344> PMID: 24247655
44. Broderick P, Chubb D, Johnson DC, Weinhold N, Försti A, Lloyd A, et al. Common variation at 3p22.1 and 7p15.3 influences multiple myeloma risk. *Nat Genet*. *Nature Publishing Group*; 2011; 44: 58–61. <https://doi.org/10.1038/ng.993> Common PMID: 22120009

45. Chubb D, Weinhold N, Broderick P, Chen B, Johnson DC, Försti A, et al. Common variation at 3q26.2, 6p21.33, 17p11.2 and 22q13.1 influences multiple myeloma risk. *Nat Genet.* Nature Publishing Group; 2013; 45: 1221–1225. <https://doi.org/10.1038/ng.2733> PMID: 23955597
46. Weinhold N, Johnson DC, Chubb D, Chen B, Försti A, Hosking FJ, et al. The CCND1 c.870G>A polymorphism is a risk factor for t(11;14)(q13;q32) multiple myeloma. *Nat Genet.* 2013; 45: 522–5. <https://doi.org/10.1038/ng.2583> PMID: 23502783
47. Swaminathan B, Thorleifsson G, Jöud M, Ali M, Johnsson E, Ajore R, et al. Variants in ELL2 influencing immunoglobulin levels associate with multiple myeloma. *Nat Commun.* 2015; 6: 7213. <https://doi.org/10.1038/ncomms8213> PMID: 26007630
48. Mitchell JS, Li N, Weinhold N, Försti A, Ali M, Duin M Van, et al. Genome-wide association study identifies multiple susceptibility loci for multiple myeloma. *Nat Commun.* 2016; 7: 12050. <https://doi.org/10.1038/ncomms12050> PMID: 27363682
49. Nie Z, Xue Y, Yang D, Zhou S, Deroo BJ, Archer TK, et al. A specificity and targeting subunit of a human SWI/SNF family-related chromatin-remodeling complex. *Mol Cell Biol.* 2000; 20: 8879–88. Available: <http://www.ncbi.nlm.nih.gov/pubmed/11073988> PMID: 11073988
50. Jones S, Wang T-L, Shih I-M, Mao T-L, Nakayama K, Roden R, et al. Frequent mutations of chromatin remodeling gene ARID1A in ovarian clear cell carcinoma. *Science.* 2010; 330: 228–31. <https://doi.org/10.1126/science.1196333> PMID: 20826764
51. Hodges C, Kirkland JG, Crabtree GR. The Many Roles of BAF (mSWI/SNF) and PBAF Complexes in Cancer. *Cold Spring Harb Perspect Med.* 2016; 6. <https://doi.org/10.1101/cshperspect.a026930> PMID: 27413115
52. Puente XS, Beà S, Valdés-Mas R, Villamor N, Gutiérrez-Abril J, Martín-Subero JI, et al. Non-coding recurrent mutations in chronic lymphocytic leukaemia. *Nature.* 2015; 526: 519–524. <https://doi.org/10.1038/nature14666> PMID: 26200345
53. Lunning MA, Green MR. Mutation of chromatin modifiers; an emerging hallmark of germinal center B-cell lymphomas. *Blood Cancer J.* 2015; 5: e361. <https://doi.org/10.1038/bcj.2015.89> PMID: 26473533
54. Choi J, Goh G, Walradt T, Hong BS, Bunick CG, Chen K, et al. Genomic landscape of cutaneous T cell lymphoma. *Nat Genet.* 2015; 47: 1–11. <https://doi.org/10.1038/ng.3188>
55. Purcell S, Neale B, Todd-Brown K, Thomas L, Ferreira MAR, Bender D, et al. PLINK: A Tool Set for Whole-Genome Association and Population-Based Linkage Analyses. *Am J Hum Genet.* 2007; 81: 559–575. <https://doi.org/10.1086/519795> PMID: 17701901
56. 1000 Genomes Project Consortium, Auton A, Brooks LD, Durbin RM, Garrison EP, Kang HM, et al. A global reference for human genetic variation. *Nature.* 2015; 526: 68–74. <https://doi.org/10.1038/nature15393> PMID: 26432245
57. Abel HJ, Thomas A. Accuracy and Computational Efficiency of a Graphical Modeling Approach to Linkage Disequilibrium Estimation. *Stat Appl Genet Mol Biol.* 2011; 10. <https://doi.org/10.2202/1544-6115.1615> PMID: 21291415
58. Matise TC, Chen F, Chen W, De La Vega FM, Hansen M, He C, et al. A second-generation combined linkage physical map of the human genome. *Genome Res.* 2007; 17: 1783–6. <https://doi.org/10.1101/gr.7156307> PMID: 17989245
59. Lauritzen SL. *Graphical models.* Clarendon Press; 1996.
60. Linderman MD, Brandt T, Edelmann L, Jabado O, Kasai Y, Kornreich R, et al. Analytical validation of whole exome and whole genome sequencing for clinical applications. *BMC Med Genomics.* 2014; 7: 20. <https://doi.org/10.1186/1755-8794-7-20> PMID: 24758382
61. Paila U, Chapman BA, Kirchner R, Quinlan AR. GEMINI: Integrative Exploration of Genetic Variation and Genome Annotations. Gardner PP, editor. *PLoS Comput Biol.* 2013; 9: e1003153. <https://doi.org/10.1371/journal.pcbi.1003153> PMID: 23874191
62. Neale BM, Rivas MA, Voight BF, Altshuler D, Devlin B, Orho-Melander M, et al. Testing for an unusual distribution of rare variants. *PLoS Genet.* 2011; 7. <https://doi.org/10.1371/journal.pgen.1001322> PMID: 21408211